PHYSICAL REVIEW E **90**, 062711 (2014)

Effective diffusion of confined active Brownian swimmers

Mario Sandoval* and Leornardo Dagdug
Department of Physics, Universidad Autonoma Metropolitana-Iztapalapa, Distrito Federal 09340, Mexico
(Received 1 July 2014; published 18 December 2014)

We theoretically find the effect of confinement and thermal fluctuations on the diffusivity of a spherical active swimmer moving inside a two-dimensional narrow cavity of general shape. The explicit formulas for the effective diffusion coefficient of a swimmer moving inside two particular cavities are presented. We also compare our analytical results with Brownian dynamics simulations and we obtain excellent agreement.

DOI: 10.1103/PhysRevE.90.062711 PACS number(s): 87.10.−e, 82.70.−y

I. INTRODUCTION

Diffusion processes of particles, molecules, or even living microorganisms are common in nature. Human metabolism, breathing, medical drug delivery, and the motion of viruses and bacteria are some examples. The fundamental physics behind these processes was elucidated for the first time in 1905, when a theory for diffusion was proposed by Einstein [1]. Since then, several works considering diffusion of free noninteracting isotropic [2,3] and anisotropic [4,5] particles, as well as the effect of external fields on the diffusion of isotropic [6–9] and anisotropic [10] particles, have been studied.

More recently, the influence of thermal forces on noninteracting active particles (driven by an assumed internal mechanism) has received considerable attention inspired from both fundamental and technological interests. On one hand, the biophysical community is trying to elucidate basic mechanisms involved in cell locomotion [11]; on the other hand, the bioengineering community is developing artificial microrobots [12,13] able to propel themselves. In this sense, isotropic self-propelled bodies subject to thermal forces [14–16] and anisotropic swimmers [15] have been analyzed in the absence and presence of external fields [17–20].

Another relevant aspect on diffusive processes is the effect of confinement on particle displacement. In nature and in many technological applications, passive (ions, molecules, cells) and active (viruses, bacteria) particles usually move under geometrical constrains (boundaries), like through ionic channels [21], membranes [22], artificial nanopores [23,24], porous media [25], microfluidic devices [26], and carbon nanotubes [27]. As one can see, confinement is mainly due to physical walls (although hydrodynamic confinement is also possible [28]) hence the necessity of including wall effects on particle diffusion.

A theoretical framework including wall effects on the diffusion of passive particles was achieved by Zwanzig [29]. Based on the idea that physical walls can be seen as entropic potentials and that effective diffusion coefficients depend on position, he derived for the first time a Smoluchowski equation for a confined passive particle. By solving this equation, an effective analytical diffusion coefficient that includes the effect of physical boundaries can be obtained. Recent work concerning the diffusion of confined, noninteracting, passive particles includes Refs. [30–33]. Confined, active, interacting particles forming stable structures due to an interplay among hydrodynamic forces and solid boundaries, due to cavities of simple shape, were recently treated by Goldstein [34,35]. Additionally, active, noninteracting particles diffusing inside cavities of more complex shape have only been computationally studied [36]. Hence theoretical work on active particles inside cavities of complex shape, to our knowledge, has not yet been reported.

In this article, we theoretically study a self-propelled particle subject to thermal fluctuations and swimming inside a two-dimensional narrow cavity of general shape. Hydrodynamic effects near the walls are neglected, as well as particle-particle interaction; the latter assumption is reasonable for a typical concentration of microorganisms in a natural suspension [37].

We derive the corresponding confined Smoluchowski equation for the probability distribution function of the particle moving inside a narrow asymmetric cavity, which we then exploit to calculate the effective swimmer diffusivity. Our theoretical results are applied to two specific cases, that is, a swimming particle moving inside a zig-zag cavity and a swimming particle inside a cavity made of circular sections. Finally, our theoretical results are validated using Brownian dynamics simulations.

II. MODEL

Consider a spherical particle of radius a, immersed in a fluid at fixed temperature T, that self-propels (swims) inside a two-dimensional asymmetric cavity of width $w(x) = A_2(x) - A_1(x)$, where $A_2(x)$ and $A_1(x)$ are, respectively, the upper and lower boundary of the cavity shape (see Fig. 1). The particle is subject to thermal fluctuations (modeled as white noise) in translation and rotation. We also impose a swimming velocity, $\mathbf{U}_s(t) = U_s(t)\mathbf{e}(t)$, where we denote by $\mathbf{e}(t) = [e_1(t), e_2(t)]$ the instantaneous unit vector in the direction of swimming with the origin at the center of the sphere and by $U_s(t)$ the instantaneous magnitude of the swimming velocity along $\mathbf{e}(t)$.

Collisions between the particle and walls are modeled as follows. For translation, we assume a mirror reflective wall, while for rotation we assume a frictionless wall that does not affect the particle orientation. For the particle description, we follow a Smoluchowski approach; hence we deal with the particle probability density function (p.d.f.) $P(\mathbf{x}, \varphi, t)$, representing the probability of locating it at position $\mathbf{x} = (x, y)$ and orientation φ at time t. Thus the corresponding two-dimensional Smoluchowski equation for P and for the case

*sem@xanum.uam.mx

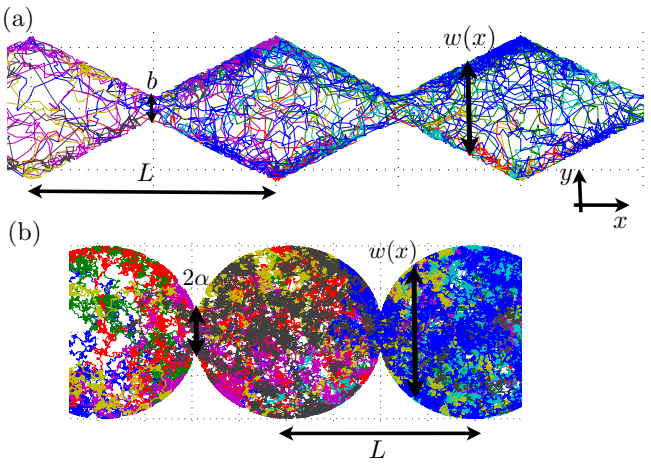

FIG. 1. (Color online) Schematics of the two studied cavities. (a) A zig-zag cavity of width $w(x)$, narrow cross-section b, and period L. (b) A semicircular cavity of width $w(x)$, radius R, period L, and narrow cross-section 2α. The cavities shown are the result of the performed Brownian simulations. Here, each color represents the followed random path of a given active particle.

of an unbounded active particle is [38,39]

$$\frac{\partial P}{\partial t} + U_s(t)\mathbf{e}(t)\cdot\nabla P = D_B\nabla^2 P + D_\Omega\frac{\partial^2 P}{\partial\varphi^2}, \tag{1}$$

where D_B is the translational diffusion coefficient ($D_B = k_BT/R_U$), D_Ω is the rotational diffusion coefficient ($D_\Omega = k_BT/R_\Omega$), and $\nabla = (\partial/\partial x,\partial/\partial y)$. Here, $R_U = 6\pi\eta a$ and $R_\Omega = 8\pi\eta a^3$ are, respectively, the viscous resistances to translation and rotation of the sphere, while η is the fluid viscosity.

III. CONFINED ACTIVE SMOLUCHOWSKI EQUATION

We start by deriving the corresponding Smoluchowski equation for the case of a confined particle swimming inside an asymmetric cavity of width $w(x)$. Following Kalinay and Percus [32,33], we project Eq. (1) along the longitudinal x direction and define the projected one-dimensional p.d.f. $G(x,\varphi,t)$ as

$$G(x,\varphi,t) = \int_{y=A_1(x)}^{y=A_2(x)} P(\mathbf{x},\varphi,t)dy. \tag{2}$$

Then, each term of Eq. (1) is integrated with respect to y from $y = A_1(x)$ to $y = A_2(x)$. After some algebra, one arrives at

$$\begin{aligned}
&\frac{\partial G}{\partial t} + U_s e_1\left[\frac{\partial G}{\partial x} + \frac{dA_1}{dx}P\Big|_{y=A_1}\right] \\
&\quad - U_s e_1\frac{dA_2}{dx}P\Big|_{y=A_2} + U_s e_2 P\Big|_{y=A_1}^{y=A_2} \\
&= D_B\frac{\partial^2 G}{\partial x^2} + D_B\frac{\partial P}{\partial y}\Big|_{y=A_1}^{y=A_2} + D_\Omega\frac{\partial^2 G}{\partial\varphi^2} \\
&\quad - D_B\frac{\partial}{\partial x}\left(\frac{dA_2}{dx}P\Big|_{y=A_2} - \frac{dA_1}{dx}P\Big|_{y=A_1}\right) \\
&\quad + D_B\frac{\partial P|_{y=A_1}}{\partial x}\frac{dA_1}{dx} - D_B\frac{\partial P|_{y=A_2}}{\partial x}\frac{dA_2}{dx}.
\end{aligned} \tag{3}$$

In order to simplify Eq. (3), we call for the boundary conditions we should impose at the walls. These boundary conditions are zero net fluxes along the walls. Hence the translational, $\mathbf{J}^t = -D_B\nabla P + U_s(t)\mathbf{e}(t)P$, and rotational, $\mathbf{J}^R = -D_\Omega\partial P/\partial\varphi\widehat{\varphi}$, fluxes must satisfy

$$\widehat{v}_u\times\mathbf{J}^t = \mathbf{0} \quad\text{and}\quad \widehat{v}_l\times\mathbf{J}^t = \mathbf{0}, \tag{4}$$

where $\widehat{v}_u = [\mathbf{i} + A_2'(x)\mathbf{j}]/\sqrt{1+A_2'(x)^2}$ is the upper unit tangent vector to the curve $y = A_2(x)$, and $\widehat{v}_l = [\mathbf{i} + A_1'(x)\mathbf{j}]/\sqrt{1+A_1'(x)^2}$ is the lower unit tangent vector to the curve $y = A_1(x)$. Here the prime denotes derivative with respect to x. Note that once Eq. (4) is satisfied, the condition of zero net flux at the walls for $\mathbf{J}^R$ is automatically satisfied. By subtracting $\widehat{v}_u\times\mathbf{J}^t - \widehat{v}_l\times\mathbf{J}^t$ one gets

$$\begin{aligned}
&D_B\frac{\partial P}{\partial y}\Big|_{y=A_1}^{y=A_2} + D_B A_1'\frac{\partial P}{\partial x}\Big|_{y=A_1} - D_B A_2'\frac{\partial P}{\partial x}\Big|_{y=A_2} \\
&\quad = U_s e_2 P|_{y=A_1}^{y=A_2} + U_s e_1[A_1'P|_{y=A_1} - A_2'P|_{y=A_2}].
\end{aligned} \tag{5}$$

The next step is to consider a very thin channel, hence

$$G = \int_{y=A_1(x)}^{y=A_2(x)} Pdy \simeq P(x,A_2(x),\varphi,t)\int_{y=A_1(x)}^{y=A_2(x)} dy; \tag{6}$$

thus we conclude that

$$\begin{aligned}
P(x,A_2(x),\varphi,t) &\simeq P(x,A_1(x),\varphi,t) \\
&= \frac{G(x,\varphi,t)}{A_2(x) - A_1(x)}.
\end{aligned} \tag{7}$$

Therefore for a thin channel $P|_{y=A_1}^{y=A_2} = 0$. Finally, substituting Eq. (5) into Eq. (3), and using Eq. (7) together with the definition of $w(x) = A_2(x) - A_1(x)$, one arrives at

$$\begin{aligned}
&\frac{\partial G}{\partial t} + U_s e_1\frac{\partial G}{\partial x} \\
&\quad = D_B\frac{\partial}{\partial x}\left[w(x)\frac{\partial}{\partial x}\left(\frac{G}{w(x)}\right)\right] + D_\Omega\frac{\partial^2 G}{\partial\varphi^2},
\end{aligned} \tag{8}$$

which is the required Smoluchowski equation for a confined active particle swimming inside an asymmetric channel, which performs both rotational and translational Brownian motion.

IV. SOLUTION OF THE CONFINED ACTIVE SMOLUCHOWSKI EQUATION

In order to find the effective diffusion of our confined swimmer, we would need to explicitly find $G(x,\varphi,t)$. However, we notice that, by setting $w(x) = 1$ into Eq. (8), we recover the one-dimensional diffusion problem of an active particle performing translational and rotational Brownian motion. Therefore, the effective diffusion coefficient, D, for the one-dimensional problem with $w(x) = 1$, and when the particle is swimming at constant speed $U_s(t) = U$, is already known [40,41], namely,

$$D = D_B + U^2/2D_\Omega. \tag{9}$$

On the other hand, if we consider the case when autopropulsion is absent, that is, $U_s(t) = 0$, and when $w(x)\neq 1$, Eq. (8) models a confined passive Brownian particle, which according

to the theory of Rubi and Reguera [30,31] provides an effective diffusion coefficient of the form

$$D = \frac{D_B}{[1 + (1/4)w'(x)^2]^{1/3}}. \tag{10}$$

There is also another expression in the literature for D [32,33] but with behavior very similar to that from Rubi and Reguera [30,31].

By physically arguing that if we confine a particle with an enhanced diffusion, $D_B + U^2/2D_\Omega$, this effective diffusion should be affected by the presence of walls in the same manner as in the passive case [see Eq. (10)]. This argument is supported by analyzing Eq. (8), where the probability G (hence its resulting diffusion) should contain the effects of activity and confinement. Therefore, we suggest that Eq. (8) provides for the case of a confined, active Brownian particle moving at constant speed, an effective diffusion coefficient of the form

$$D = \frac{D_B + U^2/2D_\Omega}{[1 + (1/4)w'(x)^2]^{1/3}}. \tag{11}$$

In order to verify Eq. (11), we apply it, in the next section, to two different cavities. We theoretically find for these cases the effective diffusion coefficient that depends on the cavity shape and the particle activity. The theoretical results are also compared with Brownian dynamics simulations.

V. SWIMMING INSIDE A ZIG-ZAG CAVITY

The simplest case is that of a self-propelled particle swimming at constant speed, $U_s(t) = U =$ constant, along the orientation vector $\mathbf{e}(t)$, inside a cavity of width $w(x)$, narrow cross-section b, and period L, as shown in Fig. 1. Within one period dependence, $w(x)$ is defined as

$$w(x) = \begin{cases} b + 2\lambda x, & 0 \leqslant x \leqslant L/2, \\ b - 2\lambda(x - L), & L/2 \leqslant x \leqslant L, \end{cases} \tag{12}$$

where λ is the cavity slope. Introducing Eq. (12) into Eq. (11), and following the results of Rubi and Reguera [30,31], one gets

$$D(x) = \frac{D_B + U^2/2D_\Omega}{(1 + \lambda^2)^{1/3}}. \tag{13}$$

Due to the periodicity of our system, $D(x)$ should also be periodic. Hence the periodic effective diffusion coefficient is given by the Lifson-Jackson formula [42]

$$D_E = \frac{1}{\langle w(x)\rangle}\left\langle \frac{1}{1/D(x)w(x)} \right\rangle, \tag{14}$$

where the brackets denote the average over a period, that is, $\langle f(x)\rangle = (1/L)\int_0^L f(x)dx$. Thus by substituting Eqs. (12) and (13) into Eq. (14) one gets

$$D_E = \left[\frac{D_B + U^2/2D_\Omega}{(1 + \lambda^2)^{1/3}}\right] \frac{2\lambda\frac{L}{b}}{\left[2 + \lambda\frac{L}{b}\right]\ln\left(1 + \lambda\frac{L}{b}\right)}, \tag{15}$$

which is the effective diffusion formula for an active confined particle.

In order to validate the latter theoretical result, we compare it with Brownian dynamics simulations. To this end, we consider a spherical swimmer of radius $a = 1$ μm, immersed in water at $T = 300$ K, swimming at speed $U_s(t) = U =$ 1 μm/s, and moving inside two different zig-zag cavities with slopes $\lambda = 0.5$ and $\lambda = 1$, respectively, both with period $L = 20$ μm. Note that the above parameters were chosen arbitrarily. The results are shown in Fig. 2 where the effective diffusion [Eq. (15)] normalized by $D_0 = D_B + U^2/2D_\Omega$ (free active diffusion) is plotted as a function of L/b (solid blue line). Brownian simulation results are shown as red circles. An excellent agreement among theory and simulations can be observed for both slopes; however, for smaller L/b, the theory fails since the simulations show that, as $L/b \to 0$, the effective diffusion tends to the free diffusion coefficient D_0 (see for example the case $\lambda = 1$). The numerical diffusion coefficient was obtained by averaging over 1000 realizations during a period of 2000 s. Error bars indicating the standard deviation are also shown in Fig. 2.

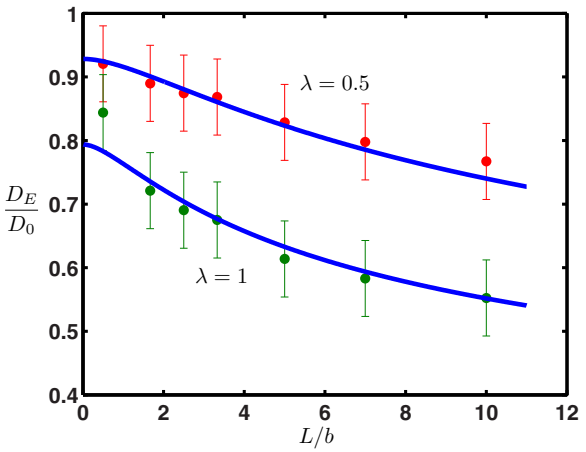

FIG. 2. (Color online) Effective diffusion coefficient D_E [Eq. (15)] for two zig-zag cavities with $\lambda = 0.5$ and $\lambda = 1$, normalized by $D_0 = D_B + U^2/2D_\Omega$ (free active diffusion), plotted as a function of L/b (solid blue line). Brownian simulation results are shown as red circles.

For illustrative purposes, we also computationally show the behavior of our active particle at short times. As it was clearly stated by ten Hagen *et al.* [15], at short times, the mean-square displacement (msd) of a self-propelled particle is affected by the initial orientation and the magnitude of its force propulsion. In our case we chose a zero initial orientation angle. Figure 3 shows the msd versus time for our active particle. We observe that at very short times the msd behaves linearly, while for a bit longer times the msd nearly behaves as $\sim t^2$. For even longer times the msd tends again to a linear behavior with respect to time as clearly shown in Fig. 3(b). Here we show a typical comparison among the theoretical (blue dashed line) and numerical (red circles) msd for a zig-zag cavity with $\lambda =$ 0.5 and $L/b = 10$.

VI. SWIMMING INSIDE A SEMICIRCULAR CAVITY

The next case of interest is an active particle swimming at constant speed, $U_s(t) = U$, along $\mathbf{e}(t)$, inside a semicircular cavity of width $w(x)$, radius R, period L, and narrow cross-section 2α (see Fig. 1). For this case, $w(x) = 2\sqrt{R^2 - x^2}$ for

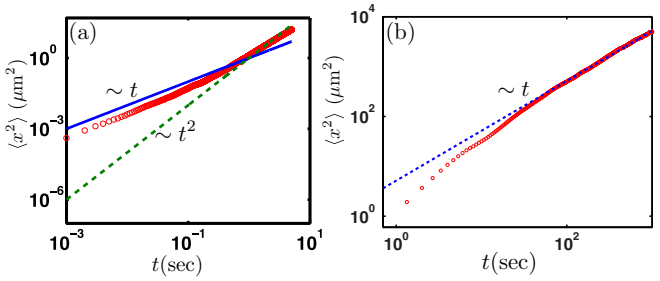

FIG. 3. (Color online) Brownian simulation results for the msd at short times. Panel (a) shows a transition of the msd with respect to time from a linear to a quadratic dependence and, finally, again to a linear dependence. Panel (b) shows the typical linear dependence of the msd with time for long times for a zig-zag cavity with $L/b = 10$.

$0 \leqslant x \leqslant L/2$. By substituting $w(x)$ into Eq. (11), one gets

$$D(x) = \left(\frac{R^2 - x^2}{R^2}\right)^{1/3} \left(D_B + \frac{U^2}{2D_\Omega}\right). \tag{16}$$

Note that for this case D explicitly depends on the x direction. By substituting Eq. (16) into Eq. (14) and after performing some integrals, one obtains the periodic effective diffusion coefficient for the semicircular cavity, namely,

$$D_E = \frac{2c^2[D_B + U^2/2D_\Omega]}{\left[\frac{\alpha c}{R} + \arcsin(c)\right] \int_0^{\arcsin(c)} \frac{d\chi}{(\cos\chi)^{2/3}}}, \tag{17}$$

where $c = \sqrt{1 - (\alpha/R)^2}$. This time the effective diffusion cannot be expressed in a closed form. Note that by setting $U = 0$ in Eq. (17), one recovers the formula for a Brownian passive particle confined in a semicircular cavity [43]. Once again, to validate our theoretical results, we compare them with Brownian dynamics simulations. We thus consider a spherical swimmer of radius $a = 1$ μm, immersed in water at $T = 300$ K, swimming at speed $U_s(t) = U = 0.5$ μm/s, and moving inside a semicircular cavity of radius $R = 10$ μm. Note that the above parameters were chosen arbitrarily. The results are shown in Fig. 4 where we plot the effective diffusion coefficient [Eq. (17)] normalized by $D_0 = D_B + U^2/2D_\Omega$, as a function of α/R (solid blue lines). Brownian simulation results are shown as red circles. Here, the diffusion coefficient was obtained by averaging over 1000 realizations during 2000 s.

Error bars giving the standard deviation are also shown in Fig. 4. Figure 4 shows an excellent quantitative agreement between the computational results and our analytical predictions. A typical comparison among the theoretical (blue dashed line) and numerical (red circles) msd for a semicircular cavity with $\alpha/R = 0.4$ is also shown in the inset of Fig. 4. The behavior of the msd for this cavity at short times is exactly the same as the one reported in Fig. 3.

VII. DISCUSSIONS

So far we have shown that our theoretical approach is in close agreement with Brownian dynamics simulations. But what happens when the magnitude of the swimming speed increases or decreases? By simulating different scenarios, each of them with different constant swimming speeds, we

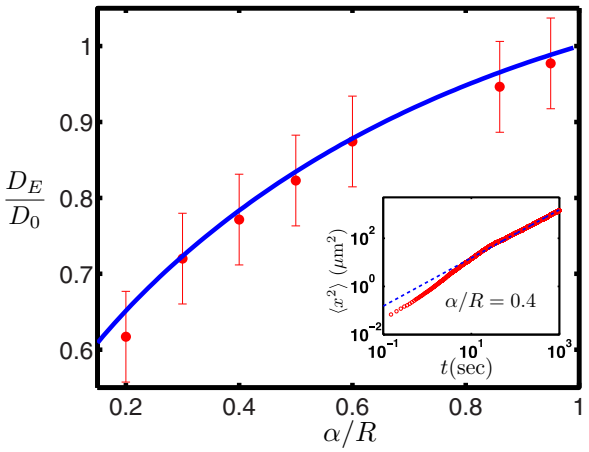

FIG. 4. (Color online) Effective diffusion coefficient D_E for a semicircular cavity [Eq. (17)] normalized by $D_0 = D_B + U^2/2D_\Omega$ (free active diffusion), plotted as a function of α/R (solid blue line). Brownian simulation results are shown as red circles. Inset: A typical comparison among the theoretical (blue dashed line) and numerical (red circles) msd of a cavity with $\alpha/R = 0.4$.

notice that, for particles inside the zig-zag cavity and with swimming speeds higher than 1 μm/s, our theory predicts a larger effective diffusion than the one obtained from our simulations. However for swimming speeds around 1 μm/s, simulation and theory are in agreement.

This situation is illustrated in Fig. 5(a) where the theoretical (solid blue lines) effective diffusion and the numerical (red circles) effective diffusion of a zig-zag cavity as a function of its width are plotted. Three different swimming speeds were chosen, namely, 0.1, 1, and 10 μm/s. Clearly our theory fails at high swimming speeds. A similar failure of our theory for the semicircular cavity occurs at high swimming speeds. This time the region of validity of our theoretical approach is reduced, since we observe that for swimming speeds higher than 0.5 μm/s our theory predicts a larger effective diffusion compared with the one obtained from our simulations. For swimming speeds around and lower than 0.5 μm/s, theory and simulations are in complete agreement. This behavior

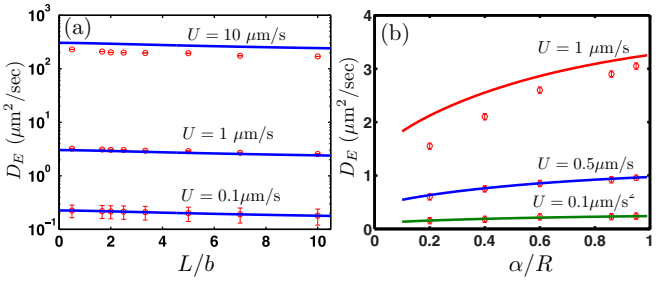

FIG. 5. (Color online) Theoretical and numerical effective diffusion coefficient D_E for a zig-zag and semicircular cavity for different swimming speeds. Panel (a) shows the results for the zig-zag cavity. Panel (b) shows the results for the semicircular cavity. In both figures, the solid lines are the theory while the red circles are the Brownian simulations results. Error bars (giving the standard deviation) in panel (a) may be smaller than the circles indicating the numerical value.

is illustrated in Fig. 5(b) where we plot the theoretical (solid lines) and numerical (red circles) effective diffusion coefficients as a function of the width of the semicircular cavity, and for three swimming speeds, namely, 0.1, 0.5, and 1 μm/s. As it has been reported [44,45], we also observe a tendency of active particles to move close to the walls rather than occupying the whole cavity [see for example Fig. 1(a)]. This effect is more noticeable in the simulations as the particle's speed increases which may be the reason for the failure of our theory at higher swimming velocities. In other words, as the particle moves faster, the information regarding the shape of the walls is lost since particles do not occupy the whole space in the cavity.

VIII. CONCLUDING REMARKS

In this article, we theoretically characterized, by using a Smoluchowski approach, the effective diffusivity of an active spherical particle subject to translational and rotational thermal forces and swimming inside a two-dimensional, narrow cavity of general shape. The deduced equations for the effective diffusion coefficient quantitatively provide the influence of confinement (walls) and activity on the diffusion of the particle. The general equations were applied to two different periodic cavities (zig-zag and semicircular cavities). For both cases a theoretical formula for the effective diffusion coefficient was deduced. To validate our theoretical results we also performed Brownian dynamics simulations that showed excellent agreement between theory and numerical experiments at moderate swimming velocities ($\sim$1 μm/s). For higher swimming velocities our theory predicts a larger effective diffusion coefficient compared with the one obtained from our simulations. This situation may be originated from a tendency of particles to accumulate at the walls as their swimming speed increases, and not to occupy the whole cavity; hence the information regarding the shape of the cavity is lost thus differing theory and simulation. Future work, and work already in progress, will be to analyze the validity of this approach for the case of a time-dependent swimming, a scenario with more realistic applications for microorganisms, since those cells tend to relax (rest) for a while and then to continue swimming [46]. Finally, this article can be seen as a theoretical extension of the work in Ref. [36].

ACKNOWLEDGMENTS

L.D. thanks Consejo Nacional de Ciencia y Tecnologia (CONACyT) Mexico for partial support under Grant No. 176452. M.S. thanks CONACyT and Programa de Mejoramiento de Profesorado (PROMEP) for partially funding this work.

[1] A. Einstein, Ann. Phys. **17**, 549 (1905).
[2] S. Chandrasekhar, Rev. Mod. Phys. **15**, 1 (1943).
[3] G. K. Batchelor, J. Fluid Mech. **83**, 97 (1977).
[4] Y. Han, A. Alsayed, M. Nobili, J. Zhang, T. C. Lubensky, and A. G. Yodh, Science **314**, 626 (2006).
[5] E. J. Hinch and L. G. Leal, J. Fluid Mech. **52**, 683 (1972).
[6] L. Ferrari, Phys. A **163**, 596 (1990).
[7] A. Zagorodny and I. Holod, Condens. Matter Phys. **3**, 295 (2000).
[8] R. T. Foister and T. G. M. van de Ven, J. Fluid Mech. **96**, 105 (1980).
[9] J. I. Jimenez-Aquino, R. M. Velasco, and F. J. Uribe, Phys. Rev. E **77**, 051105 (2008).
[10] R. Grima and S. N. Yaliraki, J. Chem. Phys. **127**, 084511 (2007).
[11] E. Lauga and T. Powers, Rep. Prog. Phys. **72**, 096601 (2009).
[12] J. Abbott, K. Peyer, M. Lagomarsino, L. Zhang, L. Dong, I. Kaliakatsos, and B. Nelson, Int. J. Rob. Res. **28**, 1434 (2009).
[13] G. Kosa, P. Jakab, G. Szekely, and N. Hata, Biomed. Microdevices **14**, 165 (2011).
[14] J. R. Howse, R. A. L. Jones, A. J. Ryan, T. Gough, R. Vafabakhsh, and R. Golestanian, Phys. Rev. Lett. **99**, 048102 (2007).
[15] B. ten Hagen, S. van Teeffelen, and H. Lowen, J. Phys.: Condens. Matter **23**, 194119 (2011).
[16] V. Lobaskin, D. Lobaskin, and I. Kulic, Eur. Phys. J. Spec. Top. **157**, 149 (2008).
[17] A. Cebers and M. Ozols, Phys. Rev. E **73**, 021505 (2006).
[18] K. Erglis, Q. Wen, V. Ose, A. Zeltins, A. Sharipo, P. Janmey, and A. Cebers, Biophys. J. **93**, 1402 (2007).
[19] B. ten Hagen, R. Wittkowski, and H. Lowen, Phys. Rev. E **84**, 031105 (2011).
[20] M. Sandoval, N. K. Marath, G. Subramanian, and E. Lauga, J. Fluid Mech. **742**, 50 (2014).
[21] B. Alberts, A. Johnson, J. Lewis, M. Raff, K. Roberts, and P. Walter, *Molecular Biology of the Cell* (Garland Science, New York, 2007).
[22] B. Hille, *Ion Channels of Excitable Membranes* (Sinauer, Sunderland, MA, 2001).
[23] Z. Siwy, I. D. Kosinska, A. Fulinski, and C. R. Martin, Phys. Rev. Lett. **94**, 048102 (2005).
[24] K. Healy, B. Schiedt, and A. P. Morrison, Nanomedicine **2**, 875 (2007).
[25] M. C. Daniel and D. Astruc, Chem. Rev. **104**, 293 (2004).
[26] A. Karimi, S. Yazdi, and A. M. Ardekani, Biomicrofluidics **7**, 021501 (2013).
[27] A. Berezhkovskii and G. Hummer, Phys. Rev. Lett. **89**, 064503 (2002).
[28] G. J. Alar Ainla and A. Jesorka, *Hydrodynamically Confined Flow Devices, Hydrodynamics—Theory and Model* (InTech, Shanghai, 2012).
[29] R. Zwanzig, J. Chem. Phys. **96**, 3926 (1992).
[30] D. Reguera and J. M. Rubi, Phys. Rev. E **64**, 061106 (2001).
[31] D. Reguera, G. Schmid, P. S. Burada, J. M. Rubi, P. Reimann, and P. Hanggi, Phys. Rev. Lett. **96**, 130603 (2006).
[32] P. Kalinay and J. K. Percus, J. Chem. Phys. **122**, 204701 (2005).
[33] P. Kalinay and J. K. Percus, Phys. Rev. E **78**, 021103 (2008).
[34] F. G. Woodhouse and R. E. Goldstein, Phys. Rev. Lett. **109**, 168105 (2012).
[35] H. Wioland, F. G. Woodhouse, J. Dunkel, J. O. Kessler, and R. E. Goldstein, Phys. Rev. Lett. **110**, 268102 (2013).
[36] P. K. Ghosh, V. R. Misko, F. Marchesoni, and F. Nori, Phys. Rev. Lett. **110**, 268301 (2013).

[37] J. P. Hernandez-Ortiz, C. G. Stoltz, and M. D. Graham, Phys. Rev. Lett. **95**, 204501 (2005).
[38] M. Enculescu and H. Stark, Phys. Rev. Lett. **107**, 058301 (2011).
[39] A. Pototsky and H. Stark, Europhys. Lett. **98**, 50004 (2012).
[40] P. S. Lovely and F. W. Dahlquist, J. Theor. Biol. **50**, 477 (1975).
[41] H. C. Berg, *Random Walks in Biology* (Princeton University Press, Princeton, NJ, 1993).
[42] S. Lifson and J. L. Jackson, J. Chem. Phys. **36**, 2410 (1962).
[43] I. Pineda, M. Vinicio-Vazquez, A. M. Berezhkovskii, and L. Dagdug, J. Chem. Phys. **135**, 224101 (2011).
[44] G. Li and J. X. Tang, Phys. Rev. Lett. **103**, 078101 (2009).
[45] K. Drescher, J. Dunkel, L. H. Cisneros, S. Ganguly, and R. E. Goldstein, Proc. Natl. Acad. Sci. USA **108**, 10940 (2011).
[46] S. Babel, B. ten Hagen, and H. Löwen, J. Stat. Mech. (2014) P02011.